THE JOURNAL OF PHYSICAL CHEMISTRY B

 VOLUME 107, NUMBER 41, OCTOBER 16, 2003

ARTICLES

Vibrational Study of the Crystalline Phases of $(CH_3(OCH_2CH_2)_2OCH_3)_2LiSbF_6$ and $P(EO)_6LiMF_6$ (M = P, As, Sb)

Roger Frech,*,† Varuni Seneviratne,‡ Zlatka Gadjourova,§ and Peter Bruce§

Department of Chemistry and Biochemistry and Department of Physics and Astronomy, University of Oklahoma, Norman, Oklahoma 73019, and School of Chemistry, University of St. Andrews, St. Andrews, Fife, KY16 9ST, U.K.

Received: February 12, 2003; In Final Form: July 24, 2003

The structure of $(CH_3(OCH_2CH_2)_2OCH_3)_2LiSbF_6$ was solved by single-crystal X-ray diffraction techniques. The compound crystallizes in the orthorhombic *Pccn* space group with a unit cell containing four lithium ions, each of which is coordinated by two $CH_3(OCH_2CH_2)_2OCH_3$ or diglyme molecules. The SbF_6^- anion does not directly interact with the cation, similar to its isolated environment in crystalline, high molecular weight $P(EO)_6LiSbF_6$. A comparative vibrational spectroscopic study of $(CH_3(OCH_2CH_2)_2OCH_3)_2LiSbF_6$ and $P(EO)_6LiSbF_6$ demonstrated that the ethylene oxide vibrations in both systems were essentially decoupled and could be analyzed in terms of a single diglyme or PEO molecule, respectively. A spectroscopic comparison of the isostructural crystalline $P(EO)_6LiAsF_6$, $P(EO)_6LiPF_6$, and $P(EO)_6LiSb_6$ compounds demonstrated that the band frequencies in the former compound are consistently higher by a few wavenumbers than those of the latter two systems. This was attributed to the effect of the Li−O distances.

1. Introduction

The ability of poly(ethylene oxide), PEO to form crystalline complexes with a variety of salts has provided a number of novel compounds in which to examine fundamental questions of structure and coordination. Addressing these fundamental questions has practical implications as well, because insight into cation−polymer and cation−anion interactions is critical to our understanding of the microscopic mechanism of ionic transport in polymer electrolytes. The interaction of the cation with the polymer is especially important because the transport of ions in the amorphous phase of PEO-based electrolytes appears to be dynamically coupled to the segmental motion of the host polymer. This motion presumably is highly dependent on the nature of the interaction between the cation and the polymer backbone.

Polymer−salt compounds whose crystal structures have been solved by X-ray diffraction techniques include $P(EO)_3LiCF_3SO_3$,[1] $P(EO)NaCF_3SO_3$,[2] $P(EO)_3NaClO_4$,[3] $P(EO)_3LiN(CF_3SO_2)_2$,[4] $P(EO)_6LiAsF_6$,[5] $P(EO)_6LiPF_6$, and $P(EO)_6LiSbF_6$.[6] In these structures the conformation of the PEO backbone is significantly and uniquely different from system to system, especially so between different polymer:salt ratios. These conformational differences reflect variations in the interaction of the cation with the polyether oxygen atoms as well as differences in chain packing requirements. The recent crystal structure solution of the compound $(CH_3(OCH_2CH_2)_2OCH_3)LiCF_3SO_3$[7] and a comparative spectroscopic study with high molecular weight $P(EO)_3LiCF_3SO_3$[8] have resulted in important insight into the nature of the interaction between the cation and

* To whom correspondence should be addressed.
† Department of Chemistry and Biochemistry, University of Oklahoma.
‡ Department of Physics and Astronomy, University of Oklahoma.
§ University of St. Andrews.

10.1021/jp030199c CCC: $25.00
Published on Web 09/20/2003

the ethylene oxide backbone in both PEO systems. In that study, we began to examine the dynamical decoupling of the ethylene oxide chain from the polyatomic anions, and further decoupling of internal motions between neighboring chains and within the chain itself.

We have now solved the crystal structure of $(CH_3(OCH_2CH_2)_2OCH_3)_2LiSbF_6$ by single-crystal X-ray diffraction techniques. In this paper, we will refer to the diethylene oxide dimethyl ether as diglyme and abbreviate it as G2. Thus the $(diglyme)_2LiSbF_6$ compound will be written as $(G2)_2LiSbF_6$. A comparative spectroscopic study of this system and its high molecular weight counterpart, $P(EO)_6LiSbF_6$, affords an excellent opportunity to develop a deeper and more general understanding of how cation−polymer interactions are reflected in the observed spectrum. In major part this is because the crystal structures of the G2−$LiSbF_6$ and PEO−$LiSbF_6$ compounds are quite different from their $LiCF_3SO_3$ analogues. The study of the diglyme− and PEO−$LiSbF_6$ compounds will be augmented by a comparative spectroscopic study of the crystalline compounds $P(EO)_6LiAsF_6$ and $P(EO)_6LiPF_6$, which are isostructural with $P(EO)_6LiSbF_6$.[6] We will address the question of whether the subtle structural differences present in these materials are manifested in their vibrational spectra.

In the unit cells of $P(EO)_6LiAsF_6$, $P(EO)_6LiPF_6$, and $P(EO)_6LiSbF_6$, there are two distorted cylinders each consisting of two PEO chains surrounding lithium ions, with the anions isolated between the cylinders.[5,6] The lack of cation−anion interactions is in marked contrast to all other polymer−salt structures studied to date in which there are significant anion−cation interactions. One of the authors has previously studied high molecular weight $P(EO)_6LiAsF_6$.[9] In that analysis, the intermolecular vibrations of the AsF_6^- ion indicated the absence of contact ion pairing between the AsF_6^- and the Li^+ ions, consistent with the reported crystal structure. The study also examined the spectral region from 800 to 1000 cm^{-1} which contains modes assigned to a mixture of predominantly CH_2 rocking and C−O stretching motions.[10] The apparent lack of coincidence in mode frequencies between the Raman and infrared spectra in that region led to the tentative conclusion that the crystallographic center of symmetry between the two polymer chains comprising a distorted cylinder played a role in the vibrational dynamics of the system. However those measurements have been repeated on a sample with a higher degree of crystallinity, and the results of the new data are incorporated in this paper.

2. Experimental Section

Lithium hexafluoroantimanate, $LiSbF_6$, (Alfa Aesar, 99%) and anhydrous 2-methoxy ethyl ether, or diglyme, (Aldrich, 99.5%) were purchased and stored in a drybox filled with nitrogen gas (VAC, <1.0 ppm of H_2O). Desired amounts of diglyme and $LiSbF_6$ were weighed and stirred until the salt is dissolved (~48 h) to make solutions characterized by their ether oxygen-to-cation ratios (O:Li). The solutions were left in the glovebox at room temperature. Very small crystals appeared after 2−3 weeks in 30:1 solution. In the lower concentrations such as 40:1 and 60:1, the crystals were seen after few months.

The crystal specimens were isolated from the 30:1 solution, and transmission IR spectra were measured from 400 to 4000 cm^{-1} on a Bruker IFS66V Fourier transform infrared (FTIR) spectrometer at a spectral resolution of 1 cm^{-1} using a KBr beam splitter. The IR samples were prepared as KBr pellets in the drybox. Raman scattering spectra were obtained in a backscattering geometry using an I.S.A. Jobin-Yvon T64000 in the triple subtractive mode with a scan time of 16 s and 10 accumulations. The 514 nm line of an argon laser operating at 300 mW measured at the laser head was used for excitation. Crystals were sealed in capillary tubes to minimize atmospheric contamination.

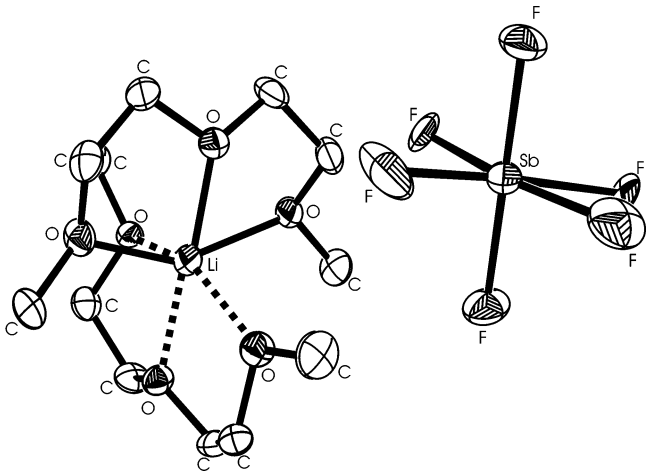

Figure 1. Coordination of a lithium ion by two G2 molecules in the crystalline $(G2)_2LiSbF_6$ compound.

The X-ray data were collected at 153(2) K on a Bruker P4 diffractometer using Mo Kα (λ = 0.710 73 Å) radiation. The data were corrected for Lorentz and polarization effects; an absorption correction was applied. The structure was solved by direct methods using the SHELXTL system and refined by full-matrix least-squares methods on F^2 using all reflections. All non-hydrogen atoms were refined anisotropically and all hydrogen atoms were included with idealized parameters.

3. Results and Discussion

3.1. Structure of $(G2)_2LiSbF_6$. The $(G2)_2LiSbF_6$ compound crystallizes in the orthorhombic *Pccn* space group (D_{2h}^{10} in Schoenflies notation) with a unit cell containing four lithium ions, each of which is coordinated by two diglyme molecules. The asymmetric unit contains one diglyme molecule, half a Li^+ cation and half a SbF_6^- anion. Therefore the unit cell contains four SbF_6^- anions and four $[Li(C_6H_{14}O_3)_2]^+$ cations. These ions are separated by 3.0−3.5 Å distances with the closest contact of 3.026(6) Å between F and C atoms. Figure 1 shows the coordination of a lithium ion by two G2 molecules; however the fluorine atoms of the SbF_6^- anion do not directly interact with the cation. There is a striking similarity between this structure and that of the high molecular weight $P(EO)_6LiAsF_6$ compound in that the latter consists of lithium ions coordinating two PEO chains with the anions relatively "free". The SbF_6^- ion is disordered in the equatorial plane. The persistence of this disorder at 153(2) K indicates that it is static rather than dynamic (see also the report of 213(2) K structure).

3.2. Comparative Vibrational Analysis of $(G2)_2LiSbF_6$ and $P(EO)_6LiSbF_6$. The SbF_6^- anions are isolated and presumably vibrate as independent entities. However our focus in this paper is on the diglyme vibrational modes in $(G2)_2LiSbF_6$ and the analogous vibrations of the PEO chain in $P(EO)_6LiSbF_6$. We are particularly interested in comparing vibrational analyses and relevant experimental data in the two compounds at various levels of vibrational decoupling.

An exact symmetry-based vibrational analysis of the $(G2)_2LiSbF_6$ compound yields the number of normal modes and their classification according to the irreducible representations of the factor group or unit cell group D_{2h}, which is isomorphous with the D_{2h}^{10} space group

$$\Gamma_{FG}[(G2)_2LiSbF_6] = 80A_g + 80B_{1g} + 82B_{2g} + 82B_{3g} + 80A_u + 79B_{1u} + 81B_{2u} + 81B_{3u} \quad (1a)$$

This equation describes the number of optical modes after subtraction of the acoustic mode contributions. The corresponding analysis of the $P(EO)_6LiSbF_6$ compound, which crystallizes in the monoclinic $P2_1/a$ or C_{2h}^5 space group, yields modes classified under the C_{2h} unit cell group

$$\Gamma_{FG}[P(EO)_6LiSbF_6] = 150A_g + 150B_g + 149A_u + 148B_u \quad (1b)$$

after subtraction of the acoustic modes.

In this paper we focus on the intramolecular vibrations of the diglyme molecules; these can be classified under the D_{2h} unit cell group as

$$\Gamma_{FG}[(G2)_2] = 63A_g + 63B_{1g} + 63B_{2g} + 63B_{3g} + 63A_u + 63B_{1u} + 63B_{2u} + 63B_{3u} \quad (2a)$$

The equation corresponding to eq 2a describing only the intramolecular vibrations of the PEO chains under the C_{2h} unit cell group is

$$\Gamma_{FG}[P(EO)_6] = 126A_g + 126B_g + 126A_u + 126B_u \quad (2b)$$

It is an interesting coincidence that there are exactly as many intramolecular PEO modes as diglyme modes. However the relative simplicity of the overall vibrational spectrum of both compounds indicates that considerable simplification in these descriptions of the modes is possible.

We now move to a level of approximation in which a degree of intermolecular coupling between molecular units is removed. In a previous study of the $(G2)_2LiCF_3SO_3$ compound, we have suggested that the modes of each dimer in that compound are highly decoupled from the modes of other dimers in the unit cell and could be analyzed according to the point group of an individual dimer. The $(G2)_2LiSbF_6$ compound also contains discrete dimers, now consisting of two diglyme molecules coordinating a single lithium ion occupying a Wyckoff site of C_2 point group symmetry. Therefore, it is of interest to examine the intramolecular vibrations of the two diglyme molecules in a single dimer. Assuming that the diglyme vibrations are coupled through the C_2 point group, a formal analysis of the irreducible representations of those modes results in

$$\Gamma_{dimer}[(G2)_2] = 63A + 63B \quad (3a)$$

It is also possible to discuss the vibrations of high molecular weight $P(EO)_6LiSbF_6$ at the same level of approximation. The unit cell of that compound contains two distorted cylinders, each consisting of two PEO chains surrounding lithium ions. The SbF_6^- ions are isolated between the cylinders with no coordinative interactions between the lithium ions and the SbF_6^- ions. We can view the two chains defining a cylinder as analogous to the two diglyme molecules in a dimer and analyze the intramolecular vibrations of the two PEO chains accordingly. Because the distorted cylinders enclose centers of symmetry, the PEO vibrations of a single cylinder can be classified under the irreducible representations of the C_i point group according to

$$\Gamma_{cylinder}[PEO] = 120A_g + 120A_u \quad (3b)$$

Within this approximation, it is important to focus on modes that will be used in this study to examine questions of vibrational decoupling. We now consider the set of modes consisting of whole body bending motions of the CH_2 units; these modes are designated as rocking (ρ), wagging (ω), and twisting (τ) modes. We also consider the internal angle deformation or "scissors" mode (δ). For each of these kinds of motion, the choice of an appropriate angle describing the motion of the CH_2 unit provides the basis for a reducible representation of the vibrational mode(s). It turns out that each of these reducible representations has the same form and consequently can be decomposed into the same set of irreducible representations. Therefore we will write just the irreducible representations for $\Gamma_{dimer}[\rho(CH_2)]$, with the understanding that $\Gamma_{dimer}[\rho(CH_2)] = \Gamma_{dimer}[\tau(CH_2)] = \Gamma_{dimer}[\omega(CH_2)] = \Gamma_{dimer}[\delta(CH_2)]$. Those irreducible representations are

$$\Gamma_{dimer}[\rho(CH_2)] = 4A + 4B \quad (4a)$$

Again focusing on the various CH_2 bending modes, the equation analogous to eq 4a for $P(EO)_6LiSbF_6$ is

$$\Gamma_{cylinder}[\rho(CH_2)] = 12A_g + 12A_u \quad (4b)$$

Here as before, $\Gamma_{cylinder}[\rho(CH_2)] = \Gamma_{cylinder}[\tau(CH_2)] = \Gamma_{cylinder}[\omega(CH_2)] = \Gamma_{cylinder}[\delta(CH_2)]$.

A further simplification is possible for both systems. If the intramolecular vibrations of a single diglyme molecule are completely decoupled, their motions have trivial symmetry and are described as

$$\Gamma[G2] = 63A \quad (5a)$$

whereas in the $P(EO)_6LiSbF_6$ compound the vibrations of a single PEO chain are also classified under trivial symmetry as

$$\Gamma[PEO] = 122A. \quad (5b)$$

We now examine the irreducible representations formed by the various CH_2 bending modes, writing those for the rocking modes as the archetypal example. In the diglyme-based compound these are

$$\Gamma[G2, \rho(CH_2)] = 4A \quad (6a)$$

and in the PEO-based compound these can be written

$$\Gamma[PEO, \rho(CH_2)] = 12A \quad (6b)$$

3.3. Experimental Data for $(G2)_2LiSbF_6$ and $P(EO)_6LiSbF_6$. We are now ready to apply the results of our analysis to the experimental data. Figure 2 shows the infrared spectra of the $(G2)_2LiSbF_6$ and $P(EO)_6LiSbF_6$ compounds in the CH_2 rocking region, $\rho(CH_2)$. Also shown for comparison are the spectra of pure diglyme and pure PEO. Figure 3 shows the corresponding Raman spectral data. Modes from 800 to 900 cm^{-1} are a mixture of CH_2 rocking and CO stretching motions.[11] The frequencies and intensities of these modes are sensitive to the coordination of the cation with the ether oxygen atoms, therefore these modes have been utilized to study the cation−polymer/oligomer interactions in ethylene oxide based systems.[12,13] In the infrared spectrum of $P(EO)_6LiSbF_6$ there are bands at 848, 831, 814, and 809 cm^{-1}, while in the Raman spectrum there are bands at 889, 865, 848, 831, 814, and 809 cm^{-1}. These data are summarized in Table 1. The coincidence of four bands in the Raman and infrared spectra strongly suggests that the vibrations in this region are *not* correlated through the center of symmetry as would be predicted by eq 4b. This equation is based on the concept that the vibrations of a PEO cylinder are correlated

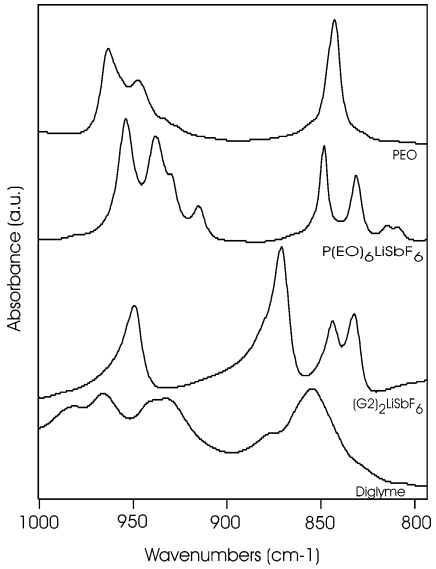

Figure 2. Infrared spectra of crystalline $(G2)_2LiSbF_6$, crystalline $P(EO)_6LiSbF_6$, pure diglyme, and pure PEO from 800 to 1000 cm^{-1}.

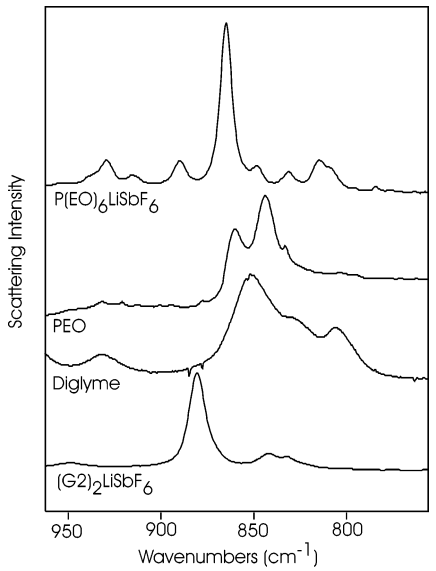

Figure 3. Raman spectra of crystalline $(G2)_2LiSbF_6$, crystalline $P(EO)_6LiSbF_6$, pure diglyme, and pure PEO from 750 to 950 cm^{-1}.

through the crystallographic inversion center. Table 1 also summarizes spectral data from the other CH_2 angle bending regions. In each region there are a number of infrared active and Raman active modes that are coincident within experimental error (estimated to be ± 1 cm^{-1}). Therefore it is clear that the intramolecular vibrations of each PEO chain comprising a cylinder are relatively decoupled from those of the other chain in the cylinder. The question now arises as to the extent of vibrational decoupling within a single PEO chain, that is, to what extent are the individual ethylene oxide units in an individual PEO chain independent? In the limit of complete decoupling, the CH_2 rocking (or twisting, wagging, etc) vibrations of an individual CH_2CH_2O unit would be

$$\Gamma[\mathrm{EO}, \rho(\mathrm{CH_2})] = 2\mathrm{A} \qquad (7)$$

An estimate of the extent to which this decoupling occurs can be obtained from eq 6b, which describes the vibrations of a single PEO chain as consisting of 12 distinct angle bending modes of each type. The selection rules predict that each mode

TABLE 1: Comparison of Infrared and Raman Frequencies (cm^{-1}) in $(G2)_2LiSbF_6$ and $P(EO)_6LiSbF_6$ in Various Spectral Regions

	$(G_2)_2LiSbF_6$		$P(EO)_6LiSbF_6$	
assignment	IR	Raman	IR	Raman
$\delta(CH)_2$	1481	1480	1485	1487
		1475 (sh)	1470	1470
	1469		1461	1460 (sh)
	1456	1456	1453	1452 (sh)
			1444	1443
$\delta(CH_3)$	1465 (sh)			
		1451		
	1448			
		1443		
$\omega(CH_2)$	1428	1427	1426 (vw)	1427 (vw)
		1398		1417
	1380	1378		1402
	1353			1392
			1374	
			1360	
			1353	
			1353	
			1347	
$\tau(CH_2)$	1280	1280		1308
	1265	1267	1302	1302
	1246	1248	1285	1285
	1237	1238		1280
				1264
			1249	1247
			1243	
				1237
$\rho(CH_2) + \nu(CO)$	880 (sh)	880		889
	871			
	844	842	848	848
	832	832	831	831
			814	814
			809	809
$\nu(CO) + \rho(CH_2)$	949	948	954	
			938	
			929	929
			915	915

is simultaneously infrared and Raman active. In both the Raman and IR spectra there are at least five distinct modes in the $\delta(CH_2)$ region, and in the Raman spectrum there are seven $\tau(CH_2)$ modes. This requires at least three and four ethylene oxide units, respectively, to contribute to the observed pattern in those regions. There are five infrared active bands in the $\omega(CH_2)$ region, requiring a minimum of three ethylene oxide units contributing to the pattern.

We can also analyze the various CH_2 bending modes of $(G2)_2LiSbF_6$ in the same manner. For an isolated G2 dimer of the $(G2)_2LiSbF_6$ compound, eq 4a predicts a total of eight modes for each type of CH_2 bending motion, whereas eq 6a predicts four modes of each type for an isolated diglyme molecule. In each case these modes are simultaneously infrared and Raman active. Referring to Table 1, it is important to note that there are four bands each in the $\omega(CH_2)$, $\tau(CH_2)$, and $\rho(CH_2)$ regions and three bands in the $\delta(CH_2)$ region. Here we do not have a mutual exclusion selection rule to guide our analysis, as in the high molecular weight PEO compound. However, the relatively low number of modes in each region and their consistency with eq 6a suggest that the vibrations of each diglyme molecule in a dimer are decoupled from the other diglyme molecule. Unfortunately, the presence of a C_2 axis rather than an inversion center as in the $(G2)_2LiCF_3SO_3$ compound makes this argument less compelling.

3.4. Comparison of $P(EO)_6LiPF_6$, $P(EO)_6LiAsF_6$, and $P(EO)_6LiSb_6$. The Raman spectra of crystalline $P(EO)_6LiPF_6$, $P(EO)_6LiAsF_6$, and $P(EO)_6LiSb_6$ in the spectral region from 800

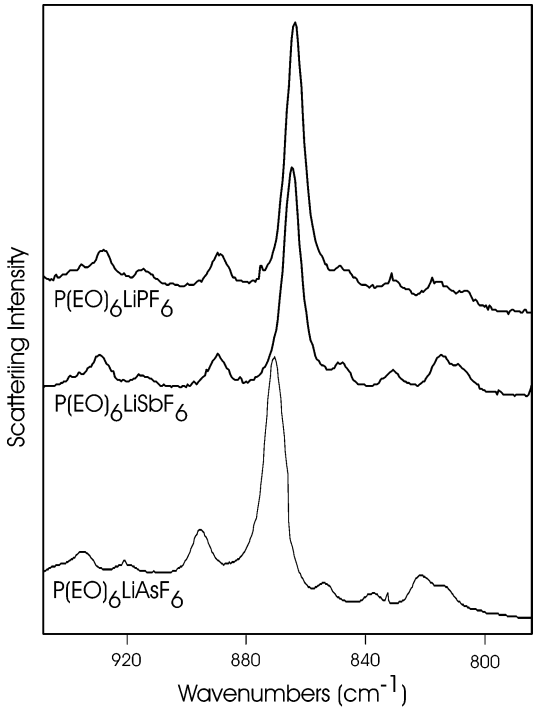

Figure 4. Raman spectra of crystalline $P(EO)_6LiPF_6$, $P(EO)_6LiAsF_6$, and $P(EO)_6LiSbF_6$ in the spectral region from 800 to 1000 cm^{-1}.

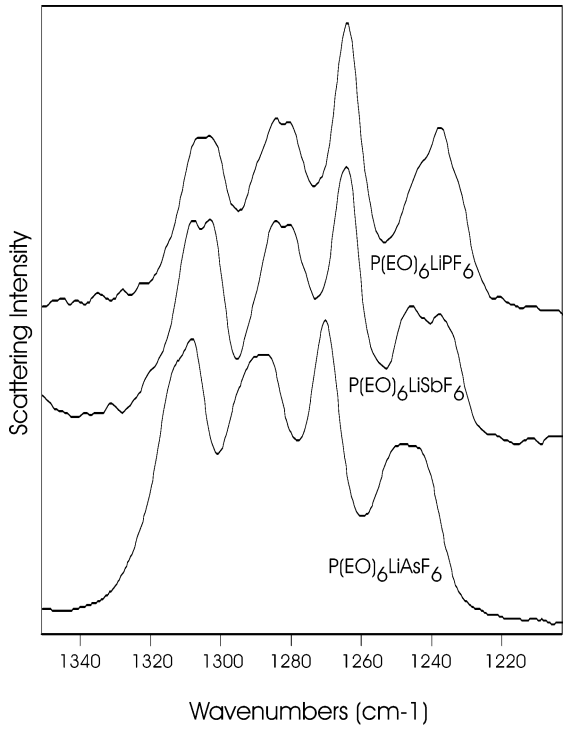

Figure 5. Raman spectra of the crystalline compounds $P(EO)_6LiPF_6$, $P(EO)_6LiAsF_6$, and $P(EO)_6LiSb_6$ in the spectral region from 1200 to 1350 cm^{-1}.

to 1000 cm^{-1} are shown in Figure 4; the frequencies of the modes are summarized in Table 2. A mode-by-mode comparison of these data establishes that the frequencies of the $P(EO)_6LiAsF_6$ compound are consistently higher by a few wavenumbers than those of the $P(EO)_6LiPF_6$ and $P(EO)_6LiSb_6$ compounds which are quite similar.

This trend continues in other spectral regions. Bands corresponding to a mixture of primarily C−O−C stretching mixed with a minor CH_2 rocking components are shown in Figure 5

TABLE 2: Comparison of Raman-Active Mode Frequencies (cm^{-1}) in Several Spectral Regions for $P(EO)_6LiMF_6$ (M = Sb, As, P)

assignment	$P(EO)_6LiSbF_6$	$P(EO)_6LiAsF_6$	$P(EO)_6LiPF_6$
$\delta(CH_2)$	1487	1491	1485
	1470	1476	1470
	1460 (sh)	1466 (sh)	1457
	1452 (sh)	1458 (sh)	1451 (sh)
	1443	1449	1440 (sh)
$\omega(CH_2)$	1427 (vw)	1424 (vw)	1427 (vw)
	1417		1417 (vw)
		1410 (vw)	
	1402 (vw)	1401	1404 (vw)
	1392		1394
$\tau(CH_2)$	1308	1314 (sh)	1307
	1302	1309	1302
	1285	1288	1284
	1280		
	1264	1271	1264
	1247	1248	1245 (sh)
	1237	1243	1238
mixed modes	1151	1156 (sh)	1149 (sh)
	1139	1144	1139
	1125	1131	1124
	1104	1109	1103
	1081	1088	1081
	1054	1059	1052
		1048 (sh)	1042 (sh)
	1038	1043	1036
	1029	1034	1028
$\nu(CO) + \rho(CH_2)$	929	935	928
	915	921	915
$\rho(CH_2) + \nu(CO)$	889	895	889
	865	870	864
	848	854	848
	831	837	831
		821	
	814	814	815
	809		806

with the frequency data summarized in Table 2. Frequencies of the CH_2 twisting mode also follow this trend, as do modes originating in the CH_2 internal deformation or "scissors" mode and mixed modes primarily involving stretching motions of the polymer backbone in the region from 1000 to 1160 cm^{-1} (Table 2).

One possible explanation might lie in the volumes of the respective unit cells, since an increase in the unit cell volume often leads to a decrease mode frequencies, all other things being equal. However the unit cell volumes are 1770, 1825, and 1890 $Å^3$ for $P(EO)_6LiMF_6$, with M = P, As, and Sb, respectively,[5,6] and clearly do not explain the similar frequencies of the P- and Sb-containing compounds and the significant difference between these and those for the As-containing compound.

The X-ray crystallographic data for these three compounds (obtained from neutron diffraction measurements) are illuminating, particularly the lithium−oxygen distances as summarized in Table 3. All of these distances are either equal or very similar in $P(EO)_6LiPF_6$ (2.17−2.18 Å) and $P(EO)_6LiSb_6$ (2.14−2.19 Å). However two of the distances in $P(EO)_6LiAsF_6$ are notably shorter (2.05 and 2.07 Å), and two are somewhat longer (2.26 and 2.28 Å). These distances are a reasonable measure of the strength of the interaction of the lithium cations with the PEO oxygen atoms. This interaction perturbs the electronic distribution in the polymer backbone, in turn affecting the frequencies and intensities of the PEO modes as seen in the spectra of Figures 4 and 5, and the data of Table 3. The striking similarity of the Li−O distances in the $P(EO)_6LiPF_6$ and $P(EO)_6LiSb_6$ compounds is then consistent with the similarity of their spectral behavior, while the relative dissimilarity of the Li−O

TABLE 3: Structural Comparison (Lengths, Å; Angles, deg) of $P(EO)_6LiMF_6$ (M=P, As, Sb) and $(G2)_2LiSbF_6$[a]

	$P(EO)_6LiPF_6$	$P(EO)_6LiAsF_6$	$P(EO)_6LiSbF_6$	$(G2)_2LiSbF_6$
$Li-O_1$	2.17	2.05	2.16	2.071
∠OCCO	−109.9	−53.6	−21.6	57.3
$Li-O_2$	2.17	2.14	2.16	2.200
∠OCCO	−58.5	−37.8	29.0	−53.5
$Li-O_3$	2.18	2.28	2.19	2.173
∠OCCO	89.5	−27.2	45.4	
$Li-O_4$	2.17	2.07	2.14	
∠OCCO	−80.3	88.3	−42.8	
$Li-O_5$	2.17	2.26	2.19	
∠OCCO	−91.2	37.9	−49.3	
$Li-O_6$				
∠OCCO	2.8	1.2	−52.4	

[a] The symbol ∠OCCO designates the $-O-C-C-O-$ dihedral angle whose end oxygen atoms are the oxygen atoms coordinated to the lithium ions indicated in the row entry immediately above and below each ∠OCCO entry. The exception is the O_6 atom, which is not coordinated to lithium ion in any of the PEO compounds. The angle given below the blank $Li-O_6$ row is the value of the $-O_6-C-C-O_1-$ Angle

distances in the $P(EO)_6LiAsF_6$ compound leads to subtle although clear spectral differences compared with the other two compounds.

4. Conclusions

A symmetry-based analysis of the number and symmetry species of vibrational modes expected in the crystalline compounds $P(EO)_6LiSbF_6$ and $(G2)_2LiSbF_6$ has been given at various levels of vibrational decoupling. Particular attention has been focused on those modes originating in the vibrations of the ethylene oxide based chain. In $P(EO)_6LiSbF_6$, the PEO chain vibrations involving CH_2 bending motions are localized to a single PEO chain, regardless of the fact that in the unit cell of the crystal two PEO chains are organized into a cylinder surrounding lithium ions. In $(G2)_2LiSbF_6$, the same level of vibrational decoupling probably occurs, i.e., the CH_2 bending motions are localized to a single G2 molecule although the G2 molecules are paired in dimers. However the evidence for this is not unambiguous as in the high molecular weight $PEO-LiSbF_6$ compound.

In a previously study of the related $(G2)_2LiCF_3SO_3$ compound, the decoupling of the two diglyme molecules in the dimer was attributed to the lack of a direct coordinative interaction between the two G2 molecules with a common lithium ion. However, in the $(G2)_2LiSbF_6$ dimer, there is a lithium ion directly interacting with the oxygen atoms of the two G2 molecules. Therefore the observation that these two G2 molecules are vibrationally decoupled argues against direct coordinative interactions being the sole determining factor in the vibrational coupling of two G2 units. Some insight into this problem is to be gained by a further comparison of the two G2-containing compounds. In the $(G2)_2LiCF_3SO_3$ dimer each lithium ion provides a direct coordinative interaction between two oxygen atoms, one from each of the two triflate ions in the dimer. The observation that the $\nu_s(SO_3)$ and $\delta_s(CF_3)$ intramolecular vibrations of the CF_3SO_3 anion were found to be correlated in the $(G2)_2LiCF_3SO_3$ dimer, whereas the G2 vibrations in the $(G2)_2LiSbF_6$ dimer are decoupled argues that the nature of the vibrational mode plays a critical role in the degree of decoupling. The vibrational induced dipole of the SO_3 unit in the triflate ion is relatively large as evidenced by the strong absorptions of $\nu_s(SO_3)$ and $\nu_{as}(SO_3)$ in the infrared spectrum. Hence the dipole−dipole coupling between the two S−O subunits whose oxygen atoms are coordinated to a common lithium ion may also be important in correlating the vibrational motion. The $\delta_s(CF_3)$ modes are correlated through electronic redistribution effects as previously noted and also reflect the coupled $\nu_s(SO_3)$ frequencies.[14]

In a comparative Raman study, the frequencies in crystalline $P(EO)_6LiAsF_6$ were found to be consistently higher by a few wavenumbers than those in $P(EO)_6LiPF_6$ and $P(EO)_6LiSb_6$ for a wide variety of vibrational modes. The effect of unit cell volume and PEO chain conformation sequence play a minimal role in this behavior. However the higher frequencies in $P(EO)_6LiAsF_6$ appear to be related to the Li−O distances, two of which are significantly longer and two of which are significant shorter in the As-containing compound.

Acknowledgment. This work was partially supported by funds from the Oklahoma Center for the Advancement of Science and Technology, Contract No. 5377, Oklahoma NASA EPSCOR (Power Generation and Storage), The Research Corporation (Grant No. RA0306), and NSF (Grant No. DMR-0072544).

Note Added in Proof. We were made aware of a recent vibrational spectroscopic study of poly(ethylene oxide):LiX complexes ($X = PF_6, AsF_6, SbF_6, ClO_4$) [Ducasse, L.; Dussauze, M.; Grondin, J.; Lassègues, J.-C.; Naudin, C.; Servant, L. *Phys. Chem. Chem. Phys.* **2003**, *5*, 567]. The authors noted that the PEO bands in the complexes were similar, with small differences attributed to orientation effects originating in crystallized regions. They have reported band frequencies averaged over the four compounds, whereas we have reported individual frequencies of the first three complexes in our Table 2. Both sets of frequency data are in general agreement.

References and Notes

(1) Lightfoot, P.; Mehta, M. A.; Bruce, P. G. *Science* **1993**, *262*, 883.
(2) Andreev, Y. G.; MacGlashan, G. S.; Bruce, P. G. *Phys. Rev. B* **1997**, *55*, 12011.
(3) Lightfoot, P.; Mehta, M. A.; Bruce, P. G. *J. Mater. Chem.* **1992**, *2*, 379.
(4) Andreev, Y. G.; Lightfoot, P.; Bruce, P. G. *J. Chem. Soc., Chem. Commun.* **1996**, 2169.
(5) MacGlashan, G. M.; Andreev, Y. G.; Bruce, P. G. *Nature* **1999**, *398*, 792.
(6) Gadjourova, Z.; Marero, D. M. y.; Andersen, K. H.; Andreev, Y. G.; Bruce, P. G. *Chem. Mater.* **2001**, *13*, 1282.
(7) Rhodes, C. P.; Frech, R. *Macromolecules* **2001**, *34*, 2660.
(8) Frech, R.; Rhodes, C. P. *Solid State Ionics* **2002**, *147*, 259.
(9) Rhodes, C. P.; Frech, R. *Macromolecules* **2001**, *34*, 1365.
(10) Matsuura, H.; Fukuhara, K. *J. Polym. Sci. B: Polym. Phys.* **1986**, *24*, 1383.
(11) Ogawa, Y.; Ohta, M.; Sakakibara, M.; Matsuura, H.; Harada, I.; Shimanouchi, T. *Bull. Chem. Soc. Jpn.* **1977**, *50*, 650.
(12) Frech, R.; Huang, W. *Macromolecules* **1995**, *28*, 1246.
(13) Petrowsky, M.; Rhodes, C. P.; Frech, R. *J. Solution Chem.* **2001**, *30*, 171.
(14) Huang, W.; Frech, R.; Wheeler, R. A. *J. Phys. Chem.* **1994**, *98*, 100.